

Interindividual variability of electromyographic patterns and pedal force profiles in trained cyclists

François Hug · Jean Marc Drouet ·
Yvan Champoux · Antoine Couturier ·
Sylvain Dorel

Accepted: 18 June 2008 / Published online: 16 July 2008
© Springer-Verlag 2008

Abstract The aim of this study was to determine whether high inter-individual variability of the electromyographic (EMG) patterns during pedaling is accompanied by variability in the pedal force application patterns. Eleven male experienced cyclists were tested at two submaximal power outputs (150 and 250 W). Pedal force components (effective and total forces) and index of mechanical effectiveness were measured continuously using instrumented pedals and were synchronized with surface electromyography signals measured in ten lower limb muscles. The intersubject variability of EMG and mechanical patterns was assessed using standard deviation, mean deviation, variance ratio and coefficient of cross-correlation (\bar{R}_0 , with lag time = 0). The results demonstrated a high intersubject variability of EMG patterns at both exercise intensities for biarticular muscles as a whole (and especially for Gastrocnemius lateralis and Rectus femoris) and for one monoarticular muscle (Tibialis anterior). However, this heterogeneity of EMG patterns is not accompanied by a so high intersubject variability in pedal force application patterns. A very low variability in the three mechanical profiles (effective force, total force

and index of mechanical effectiveness) was obtained in the propulsive downstroke phase, although a greater variability in these mechanical patterns was found during upstroke and around the top dead center, and at 250 W when compared to 150 W. Overall, these results provide additional evidence for redundancy in the neuromuscular system.

Keywords Pedaling · Heterogeneity · Mechanical · Electromyography · Muscle · Redundancy

Introduction

Variability in human movement has been the focus of numerous studies across multiple disciplines within the movement sciences. It is well documented that the nervous system has multiple ways of accomplishing a given motor task (Bernstein 1967). At the muscle level, there are multiple synergists as well as various combinations of agonist/antagonists that can contribute to the same end-effector trajectory and force pattern (van Bolhuis and Gielen 1999). This motor redundancy suggests that the nervous system could use different muscle activation patterns for a given movement.

Cycling task represents a typical multijoint movement characterized by several degrees of freedom. In contrast with other movements, the constant circular trajectory of the pedal constrains lower extremity displacement. Despite that, some studies have reported a high variability of electromyographic (EMG) patterns even when in trained cyclists (Ryan and Gregor 1992; Hug et al. 2004). Ryan and Gregor (1992) showed two distinct EMG patterns for the biceps femoris muscle within a population of 18 experienced cyclists (no other details about the training status of the subjects were mentioned). This study also pointed out

F. Hug · A. Couturier · S. Dorel (✉)
Research Mission, Laboratory of Biomechanics and Physiology,
National Institute for Sports and Physical Education (INSEP),
11 Avenue du Tremblay, 75012 Paris, France
e-mail: sylvain.dorel@insep.fr

F. Hug
Laboratory “Motricity, Interactions, Performance” (EA 4334),
University of Nantes, Nantes Atlantic Universities,
44000 Nantes, France
e-mail: francois.hug@univ-nantes.fr

J. M. Drouet · Y. Champoux
VélUS Group, Department of Mechanical Engineering,
Université de Sherbrooke, Sherbrooke, QC J1K2R1, Canada

interindividual differences of the EMG patterns of ten lower limb muscles, especially apparent for biarticular muscles compared to monoarticular ones. Using two complementary techniques (surface EMG and functional magnetic resonance imaging) and using only quantitative analysis (i.e., mean RMS values across seven crank revolutions), Hug et al. (2004) confirmed these results showing that the high degree of expertise of professional road cyclists is not linked to the production of a common activation pattern of lower limb muscles. Striking differences in the level of activation among these expert cyclists were also observed for biarticular muscles: rectus femoris and semimembranosus.

From a mechanical standpoint, it is interesting to note that, for a given power output–pedaling rate combination, the effective force (or torque) profile as a function of the crank angle appears to be stereotypical (Gregor et al. 1985; van Ingen Schenau et al. 1992; Sanderson et al. 2000). On the other hand, it has been suggested that substantial differences exist between subjects regarding their power generation techniques (Gregor et al. 1991). To characterize the biomechanics of force application, it is important to note that the effective force (i.e., that which acts perpendicular to the bicycle crank and thus drives the crank around in its circle) represents only one component of the total force produced at the shoe/pedal interface. On the sagittal plane, a second ineffective component of the resultant force acts along the crank, and thus performs no useful external work (Fig. 1, Hull and Davis 1981). Instrumented pedals developed since 1970s (Dal Monte et al. 1973) offer the possibility of determining both components and allow the index of mechanical effectiveness (IE), defined as the ratio of the effective force to the total force exerted by the foot on the pedal (LaFortune and Cavanagh 1983), to be calculated. However, there is a lack of information concerning the intersubject variability of the index of mechanical

effectiveness and total resultant force throughout the cycle. Finally, to our knowledge, no previous study has focused on the putative interindividual differences in all of these mechanical profiles as well as on the EMG patterns of the main lower limb muscles in the same population.

Thus, the purpose of the present study was to determine whether the relatively high interindividual variability in EMG patterns during pedaling is accompanied by variability in the pedal force application patterns. It was hypothesized that, in a population of trained cyclists, forces and IE profiles would exhibit a lower intersubject variability compared to EMG patterns. Cyclists were tested at two submaximal power outputs (i.e., 150 and 250 W). Pedal force components were measured continuously using instrumented pedals and were then synchronized with surface electromyography signals measured in ten lower limb muscles.

Methods

Subjects

Eleven male experienced cyclists whose anthropometrical and physiological characteristics are presented in Table 1 volunteered to participate in this study. The subjects had 8.5 ± 3 years of competitive experience. During the last season before the experimentation, they have covered an average of $14,000 \pm 4,333$ km. None of them had recent or ancient pathology of lower limb muscles or joints. They were informed of the possible risk and discomfort associated with the experimental procedures before they gave their written consent to participate. The experimental design of the study was approved by the Ethical Committee of Saint-Germain-en-Laye (acceptance no. 06016) and was done in accordance with the Declaration of Helsinki.

Exercise protocol

The testing protocol consisted of two sessions conducted in the following order: (1) incremental cycling exercise

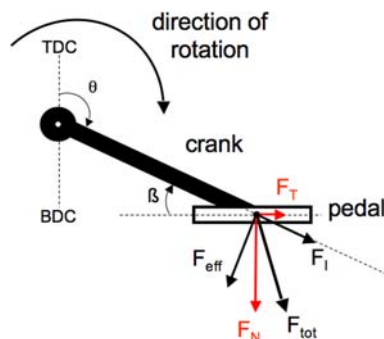


Fig. 1 Representation of the various forces applied on the pedal on a sagittal plane. Total force (F_{tot}) produced at the shoe/pedal interface is decomposed into two components: **a** effective force (F_{eff}) acts perpendicular to the bicycle crank and thus drives the crank around in its circle; **b** ineffective component (F_I) acts along the crank, and thus performs no useful external work. F_T and F_N , tangential and normal components of F_{tot} on the pedal

Table 1 Anthropometric and physical characteristics of the subjects

	Mean \pm SD	CV
Age (years)	20.5 \pm 3.4	0.166
Height (cm)	180.6 \pm 5.9	0.033
Body mass (kg)	68.5 \pm 6.6	0.096
BMI (kg m^{-2})	21.0 \pm 2.1	0.100
$\dot{V}O_{2max}$ ($\text{mL min}^{-1} \text{kg}^{-1}$)	67.1 \pm 9.2	0.137
MPT (Watts)	410.9 \pm 30.1	0.073
MAP (Watts)	391.0 \pm 22.3	0.057

BMI body mass index, CV Coefficient of variation, MPT maximal power tolerated, MAP maximal aerobic power, $\dot{V}O_{2max}$ maximal oxygen uptake

performed until exhaustion to characterize the population in terms of physical and physiological capacities; (2) experimental session consisting of two submaximal pedaling exercises.

During the first visit, in the 2 weeks preceding the experimental session, each subject performed an incremental cycling exercise (workload increments of 25 W min^{-1} ; starting at 100 W) during which the usual respiratory and ventilatory parameters were measured breath-by-breath (K4B2, Cosmed[®], Italy). The first power output achieved when the maximal oxygen uptake was reached ($\dot{V}O_{2\text{max}}$) was referred as the maximal aerobic power (MAP). Maximal power tolerated (MPT) was referred as the last stage entirely completed.

During the second session, subjects were asked, after a 10 min warm-up at 100 W, to pedal at 150 W for 6 min. This bout was immediately followed by a second one performed at 250 W for 3 min. Because of the training status of the subjects, the low workload level (i.e., 150 and 250 W representing about 38 and 63% of MAP, respectively) and the short duration of the exercises, this protocol was considered as nonfatiguing. For each of these two intensities, subjects were asked to keep a constant pedaling rate fixed at 95 rpm (± 5 rpm). This value was chosen, because it represents the mean pedaling rate (94.6 ± 4.2 rpm) freely adopted by the subjects at the end of the warm-up of the incremental cycling exercise. One among the twelve cyclists (initially enrolled in the study) has not been included in this second session due to his higher pedaling rate (>2 SD from the mean). Surface electromyography and mechanical parameters were continuously recorded during this experimental session.

Material and data collection

Subjects exercised on an electronically braked cycle ergometer (Excalibur Sport, Lode[®], Netherlands) equipped with standard crank (length = 170 mm) and with instrumented pedals described below. During both sessions, vertical and horizontal positions of the saddle, handlebar height and stem length were set to match the usual racing position of the participants (i.e., dropped posture).

A pedal dynamometer specifically designed for pedaling load measurements by VélUS group (Department of Mechanical Engineering, Sherbrooke University, Canada) was used to collect mechanical data. The instrumented pedal is compatible with LOOK CX7 clipless pedal using LOOK Delta cleat. The sagittal plane components of the total reaction force (F_{tot}) applied at the shoe/pedal interface were measured by using a series of eight strain gauges located within each pedal. F_{tot} was calculated from the measured Cartesian components (F_T , F_N) corresponding for the pedal to the horizontal forward and vertical upward forces,

respectively (Fig. 1). Static calibration was performed by applying sequentially three degrees of freedom force and moment loads to measure the direct sensitivity (F_T and F_N) and both the calibratable and noncalibratable cross-sensitivity (Rowe et al. 1998). The maximum nonlinearity for both measured components is less than 0.4% full scale (FS) and the maximum hysteresis is less than 0.8% FS. Calibration revealed an error less than 0.7% FS when only the measured force components were applied. Application of unmeasured load components created an error less than 0.8% FS. An optical encoder with a resolution of 0.4° mounted on the pedal measured pedal angle (β) with respect to the crank orientation. A zero adjustment for both components of force and pedal angle was done before each session. The crank angle (θ) was calculated based on TTL pulses delivered each 2° by the cycle ergometer. Additional TTL pulse permitted to detect the bottom dead center of the right pedal (i.e., BDC: lowest position of the right pedal with crank arm angle = 180°). All these data were digitized at a sampling rate of 2 kHz (USB data acquisition, ISAAC instruments[®], Québec, Canada) and stored on a computer.

Surface EMG activity was continuously recorded for the following ten muscles of the right lower limb: gluteus maximus (GMax), semimembranosus (SM), biceps femoris (BF), vastus medialis (VM), rectus femoris (RF), vastus lateralis (VL), gastrocnemius medialis (GM) and lateralis (GL), soleus (SOL) and tibialis anterior (TA). A pair of surface Ag/AgCl electrodes (Blue sensor, Ambu[®], Denmark) was attached to the skin with a 2 cm interelectrode distance. The electrodes were placed longitudinally with respect to the underlying muscle fibers arrangement and located according to the recommendations by SENIAM (Surface EMG for Non-Invasive Assessment of Muscles) (Hermens et al. 2000). Prior to electrode application, the skin was shaved and cleaned with alcohol to minimize impedance. The wires connected to the electrodes were well secured with adhesive tape to avoid movement-induced artifacts. Raw EMG signals were preamplified close to the electrodes (gain 375, bandwidth 8–500 Hz), and simultaneously digitized with BDC TTL pulses at a sampling rate of 1 kHz (ME6000P16, Mega Electronics Ltd[®], Finland).

Data processing

All data were analyzed with two custom-written scripts (Matlab, MathWorks[®], USA, for mechanical data; and Origin 6.1, OriginLab Corporation[®], USA, for EMG data and final processing). All mechanical data were smoothed by a 10 Hz third-order Butterworth low pass filter. Based on components F_N and F_T and pedal angle (β), F_{tot} was calculated by trigonometry and resolved into two components: one orthogonal to the crank (effective force F_{eff}) and another along the crank (ineffective force F_I). Instantaneous

index of mechanical effectiveness (IE) was determined as the ratio of the effective force to the total applied force at each point in the pedaling cycle (Sanderson 1991; Sanderson and Black 2003). A high pass filter (20 Hz) was applied on the EMG signals (Chart 5.4, AD instruments®, Hasting, UK) to diminish movement artifacts. EMG data were root-mean-squared (RMS) over a 25 ms moving window to produce linear envelope for each muscle activity pattern.

The BDC TTL pulses were used to synchronize EMG and mechanical signals of the right pedal. According to the procedure previously described (Dorel et al. 2008a, b), all data were smoothed, resampled (one value each one degree) and averaged over 30 consecutive pedaling cycles to get a representative mechanical profile (pedal forces and IE) and EMG RMS linear envelope for each muscle, each subject and each condition (i.e., 150 and 250 W). These values were expressed as a function of the crank arm angle as it rotated from the highest pedal position (0°, top dead center, TDC) to the lowest (180°, bottom dead center, BDC) and back to TDC to complete a 360° crank cycle. Except for the index of effectiveness (which is already expressed as a percentage), all the mechanical and EMG patterns were then normalized to the mean value calculated over the complete pedaling cycle as advised by various authors (Yang and Winter 1984; Shiavi et al. 1986, 1987; Burden et al. 2003). Finally, mean ensemble curves of EMG and mechanical patterns were calculated over the 11 subjects from these individual normalized patterns.

Assessment of interindividual variability

Measurements of the standard deviation (SD) of the mean ensemble curves have been used to define the amount of interindividual variability of the EMG and mechanical patterns as previously done for other locomotive patterns (Winter and Yack 1987; Ryan and Gregor 1992; Dingwell et al. 1999). The larger the distance between the mean + SD curve and the mean curve, the greater the variability in the EMG/mechanical pattern. Variability among subjects was also estimated calculating mean deviation (MD, Eq. 1) and variance ratio (VR, Eq. 2) over the complete cycle according to the following equations:

$$MD = \frac{\sum_{i=1}^k |\sigma_i|}{k} \quad (1)$$

$$VR = \frac{\sum_{i=1}^k \sum_{j=1}^n (X_{ij} - \bar{X}_i)^2 / k(n-1)}{\sum_{i=1}^k \sum_{j=1}^n (X_{ij} - \bar{X})^2 / (kn-1)} \quad (2)$$

with $\bar{X} = \frac{1}{k} \sum_{i=1}^k \bar{X}_i$ where k is the number of intervals over the pedaling cycle (i.e., 360), n is the number of participants (i.e., 11), \bar{X}_i is the mean of the normalized EMG/mechanical values obtained at the i th interval calculated

over the eleven participants, σ_i is the standard deviation of the normalized EMG/mechanical values about \bar{X}_i and X_{ij} is the normalized EMG/mechanical value at the i th interval for the j th participant.

In addition to MD, VR has been recently reported as an alternative interesting index for assessing intrasubject and intersubject variability (Burden et al. 2003; Rouffet and Hautier 2007). The lower the MD and VR values are, the lesser the variability in the EMG/mechanical patterns is.

In addition to this overall analysis, one of these indexes (i.e., VR) was also calculated for four functional angular sectors over the entire pedaling cycle (by adjusting the k value) to identify regions of greatest variability. For mechanical data, the following sectors were chosen: sector 1 represented 330°–30°; sector 2, 30°–150°; sector 3, 150°–210°; sector 4, 210°–330° (Fig. 2). From a functional point, sectors 1 and 3 correspond, respectively, to the top and bottom dead centers; sectors 2 and 4 correspond, respectively, to the main propulsive and recovery phases. Assuming a relatively constant delay (called electromechanical delay, EMD) of 50 ms (Cavanagh and Komi 1979) between the electrical event (i.e., EMG activity) and the related mechanical output (i.e., force), the angular sectors used for EMG data were shifted 28° earlier (i.e., the crank angular displacement due to EMD at 95 rpm): sector 1 represented 302°–2°; sector 2, 2°–122°; sector 3, 122°–182°; sector 4, 182°–302° (Fig. 2). This shift for EMG data due to the EMD permits to compare the same functional sectors between EMG and mechanical data as recommended by Vos et al. (1990).

Cross-correlation has been used as a method for objectively comparing the timing and shape of two EMG or mechanical patterns (Li and Caldwell 1999; Wren et al. 2006; Dorel et al. 2008a, b). The coefficient of cross-correlation (\bar{R}_0 , with lag time = 0) was determined for each

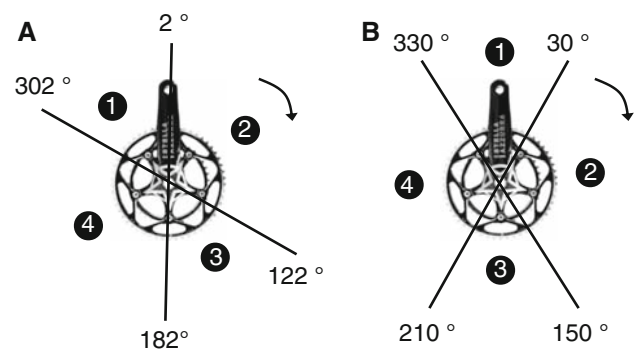


Fig. 2 Representation of the different angular sectors used for EMG (a) and mechanical (b) analysis. To compare the same (or approximately the same) functional sectors between EMG and mechanical data, angular sectors used for EMG take into account an electromechanical delay (i.e., 50 ms)

pair of individual EMG patterns obtained for a given muscle and each pair of mechanical curves (i.e., number of combination: ${}_n C_2 = {}_{11} C_2 = 55$). Thus, in the perspective to characterize interindividual variability, a mean cross-correlation coefficient was calculated ($\overline{R_0}$ average of the 55 values) for each muscle and each mechanical variable (i.e., effective force, total force and index of mechanical effectiveness). Changing the magnitude of the curves without changing their shape does not affect $\overline{R_0}$. Higher $\overline{R_0}$ values indicated less variability in the shape and timing of the

EMG/mechanical patterns (e.g., $\overline{R_0} = 1$ means that curves would exhibit exactly the same shape and timing).

Results

Average (\pm SD) EMG patterns for the ten muscles investigated are depicted in Figs. 3 and 4 (150 and 250 W, respectively). High interindividual variability is evident, especially for two biarticular muscles (GL and RF) and one

Fig. 3 RMS EMG envelope for ten lower limb muscles obtained during pedaling at 150 W. Each profile represents the mean (solid line) and the mean + standard deviation (broken line) obtained from averaging individual data across 30 consecutive pedaling cycle, normalizing to the mean RMS calculated over the complete pedaling cycle and further averaging across the 11 cyclists. *GMax* gluteus maximus, *SM* semimembranosus, *BF* biceps femoris, *VM* vastus medialis, *RF* rectus femoris, *VL* vastus lateralis, *GM* gastrocnemius medialis, *GL* gastrocnemius lateralis, *SOL* soleus, *TA* tibialis anterior. Vertical lines define the four angular sectors: *sector 1* (302°–2°), *sector 2* (2°–122°), *sector 3* (122°–182°), *sector 4* (182°–302°)

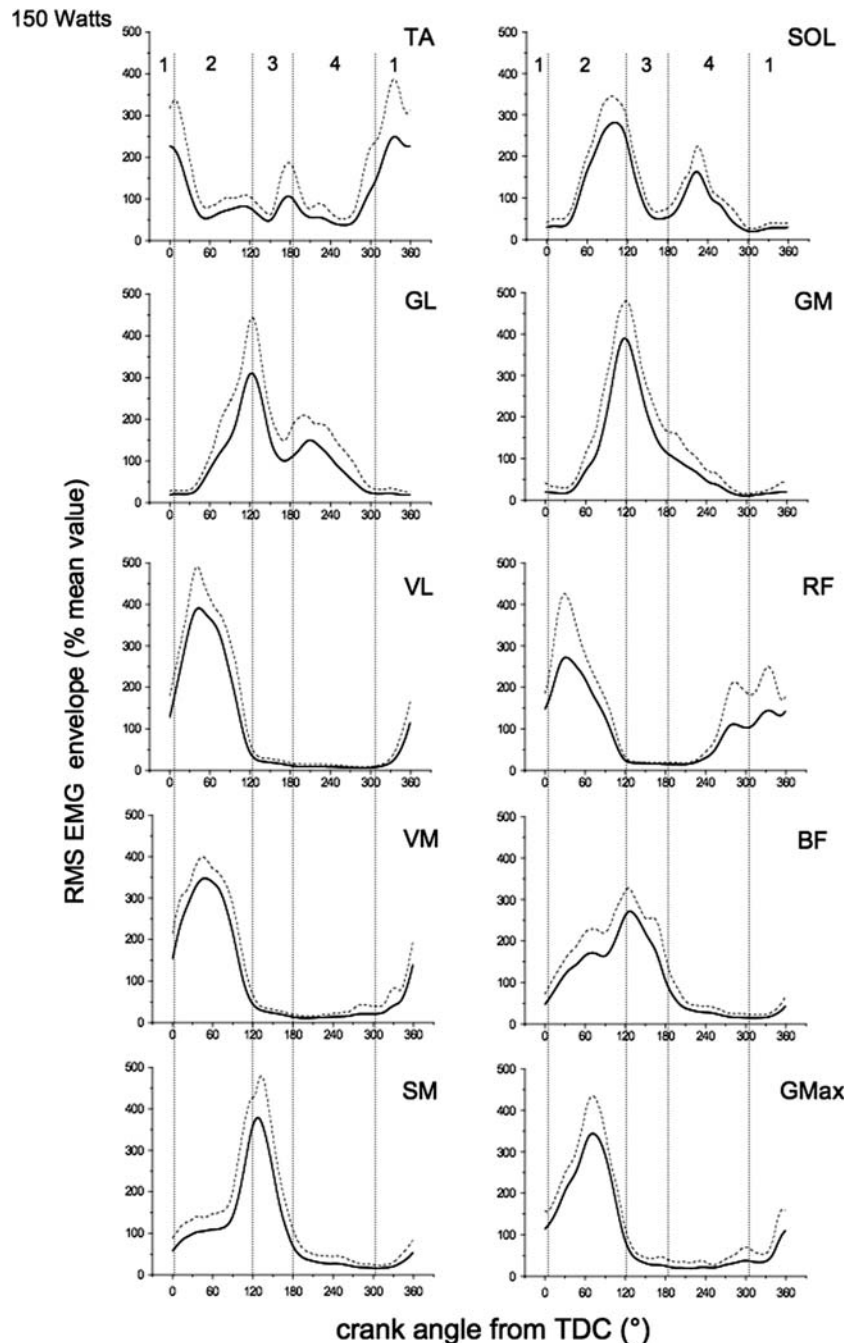
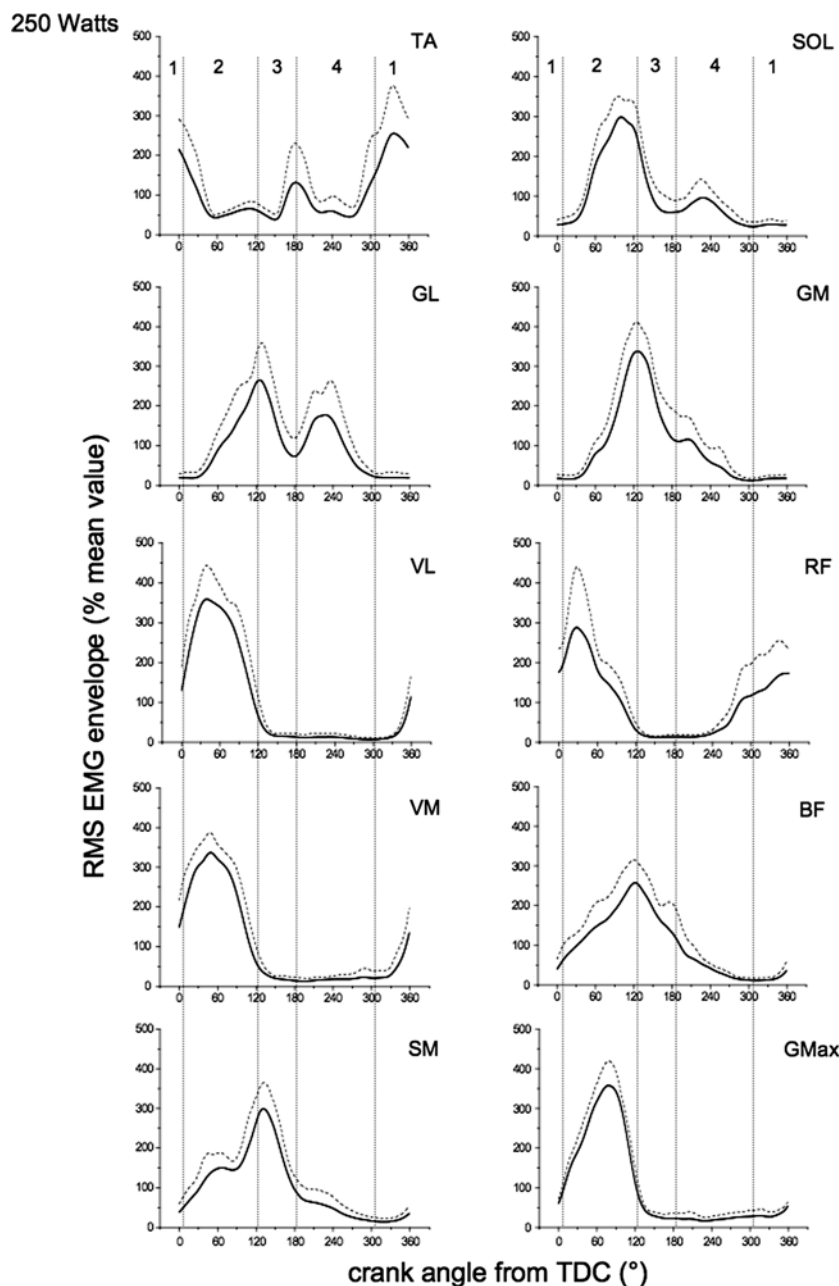


Fig. 4 RMS EMG envelope for ten lower limb muscles obtained during pedaling at 250 W. Each profile represents the mean (solid line) and the mean + standard deviation (broken line) obtained from averaging individual data across 30 consecutive pedaling cycle, normalizing to the mean RMS calculated over the complete pedaling cycle and further averaging across the 11 cyclists. *GMax* gluteus maximus, *SM* semimembranosus, *BF* biceps femoris, *VM* vastus medialis, *RF* rectus femoris, *VL* vastus lateralis, *GM* gastrocnemius medialis, *GL* gastrocnemius lateralis, *SOL* soleus, *TA* tibialis anterior. Vertical lines define the four angular sectors: *sector 1* (302°–2°), *sector 2* (2°–122°), *sector 3* (122°–182°), *sector 4* (182°–302°)

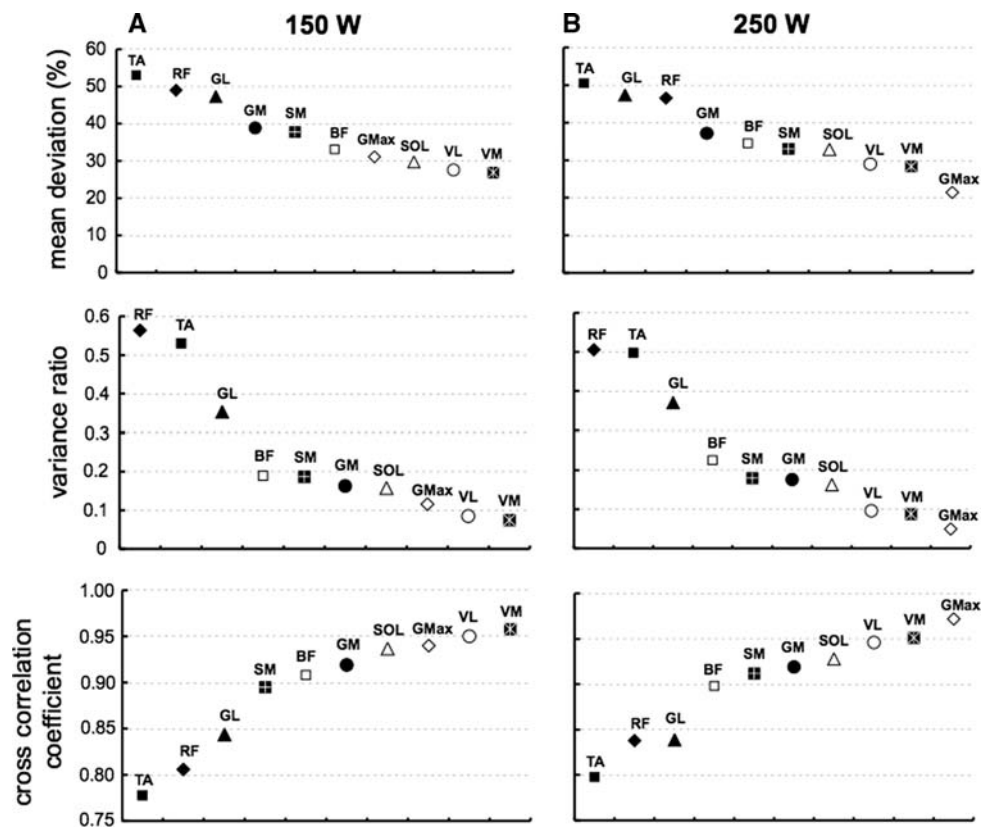


monoarticular muscle (TA). Overall, this result is confirmed by the lowest $\overline{R_0}$ and highest MD and VR for these three muscles (Fig. 5). Figure 6 depicts an example of two different patterns found in TA. Medium variability appeared for the three other biarticular muscles (BF, SM and GM). In contrast, low interindividual variability was found for the four monoarticular muscles (GMax, SOL, VL, VM) for which lower MD and VR and higher $\overline{R_0}$ values were observed. Detailed analysis for the different sectors described in Table 2 confirmed the high variability of RF and TA during their period of higher activity (i.e., sectors 1 and 2). With the exception of these muscles and to a lesser extent BF, the interindividual variability in sector 2 was relatively low

for all other muscles and especially for GMax, SOL, VL and VM, which were greatly activated during this period. GL and BF depicted a non-negligible variability in sector 3 (i.e., during higher activity period) and also in sector 4. The other muscles, which were activated to some extent in sector 4, also exhibited a medium (GM, GL, RF) to high (SOL, TA) interindividual variability.

Average (\pm SD) effective force, total force and IE profiles are depicted in Fig. 7. As shown in Table 3, the ensemble-averaged mechanical profiles show lower variability than EMG patterns as confirmed by lower MD (ranging from 7.7 to 33.3%), lower VR (ranging from 0.017 to 0.088) and higher $\overline{R_0}$ (ranging from 0.922 to

Fig. 5 Interindividual variability of complete cycle EMG RMS patterns for the ten muscles at both exercise intensities (**a** 150 W, **b** 250 W). *GMax* gluteus maximus, *SM* semimembranosus, *BF* biceps femoris, *VM* vastus medialis, *RF* rectus femoris, *VL* vastus lateralis, *GM* gastrocnemius medialis, *GL* gastrocnemius lateralis, *SOL* soleus, *TA* tibialis anterior



0.988). A very low VR value (0–0.086) for the three mechanical profiles (F_{eff} , F_{tot} and IE) was obtained in sector 2 corresponding to the propulsive downstroke phase (Table 4). F_{eff} was also very stable in sector 3 and became more variable in sector 4 and to a lesser extent in sector 1. F_{tot} presented medium interindividual variability during the three other sectors (especially in sector 3). In addition to the sector 2, IE also exhibited a very low to negligible interindividual variability in sectors 3 and 4. In contrast, a medium variability was apparent in sector 1.

Discussion

This is the first study to report on both EMG and pedal force variability in the same trained population. It shows high intersubject variability of EMG patterns at both exercise intensities (i.e., 150 and 250 W) for biarticular muscles as a whole (and specifically for GL and RF) and for one monoarticular muscle (TA). However, this heterogeneity of EMG patterns is not accompanied by a so high intersubject variability of pedal force application patterns.

Methodological aspects

EMG patterns of lower limb muscles during pedaling can be influenced by numerous factors such as power output,

pedaling rate, body position, shoe–pedal interface and training status (for a review, see Hug and Dorel 2008). For this reason, all of these parameters were standardized. To allow appropriate comparisons between individuals, EMG patterns were normalized with respect to the mean value calculated over the complete cycle in line with numerous previous studies focusing on gait analysis (Winter and Yack 1987; Burden et al. 2003). However, it should be noted that this normalization procedure only provides information about the level of muscle activity in relation to the average activity over the pedaling cycle (i.e., shape of the EMG pattern). Thus, in contrast with methods referring to the isometric maximal voluntary contraction or the force–velocity test, this procedure does not allow to provide information on the absolute level of muscle activity required during pedaling. As these latter methods remain criticized on the basis of possible misinterpretations (Mirka 1991), the present study focused only on the intersubject variability in the shape and timing of EMG patterns over the pedaling cycle, in the same way as previous studies (Ryan and Gregor 1992; van Ingen Schenau et al. 1992; Chapman et al., 2007). Obviously, it would not seem appropriate to designate EMG variability as “high” in a muscle that is essentially not active at all. However, all the ten muscles recorded in this study showed a distinct phasic activity (Fig. 3) and were chosen for their role in the pedaling task as previously shown by various authors (Ericson 1986; Shan 2008).

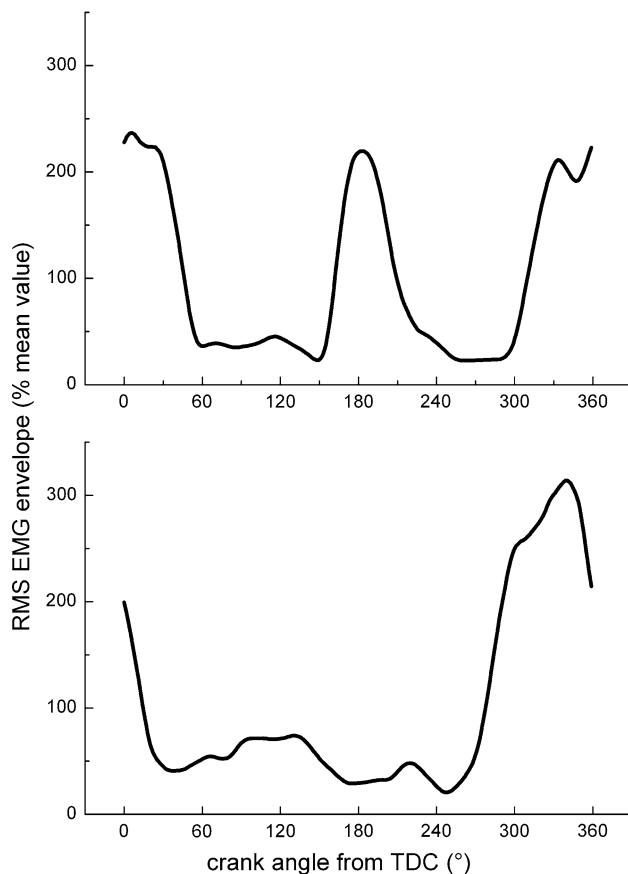


Fig. 6 Example of two different patterns observed for the tibialis anterior muscle. Each profile represents the mean obtained from averaging individual data across 30 consecutive pedaling cycles, normalizing to the mean RMS calculated over the complete pedaling cycle

Traditionally, the coefficient of variation (CV) allows the variability of a data set with a larger mean and a larger standard deviation to be compared with the variability of a data set with a smaller mean and associated with a smaller standard deviation (Ryan and Gregor 1992; Hug et al. 2004). However, CV is influenced greatly by the mean EMG value (i.e., denominator of CV formula) and could be overestimated in the sectors in which the muscle is not activated or is weak (e.g., between 180° and 300° for VL). For this reason, we chose to calculate MD and the variance ratio as recently proposed by Burden et al. (2003). The cross-correlation coefficient (with lag time = 0) were also calculated to compare the shape and timing of the individual EMG patterns as recently suggested by Wren et al. (2006). In the present study, this latter index was originally used to determine a robust mean cross correlation value (\bar{R}_0) considering all possible trial pairs to assess the intersubject variability. Finally, the advantage of this method was to be insensitive to signal amplitude and hence to provide a coefficient unaffected by this normalization procedure.

EMG patterns

Since considerable discussion is possible in view of the detailed EMG profiles depicted in Figs. 3 and 4, only major results will be discussed. A recent study (Dorel et al. 2008b) aimed to assess intrasession repeatability of EMG curves for ten lower limb muscles between two submaximal pedaling exercises (workload fixed at 150 W) performed before and after a 53-min simulated training session. Coefficients of cross-correlation ranging from 0.942 to 0.988 were reported. Interestingly, in the present study, for each muscle, at both 150 and 250 W, the calculated coefficient of cross-correlation (Fig. 5) is lower than those reported by Dorel et al. (2008b) suggesting that intersubject variability is higher than intrasession variability. However, it is noteworthy that muscles exhibiting the greater intersubject variability are the same as those exhibiting greater intraindividual variability.

Few studies have previously focused on heterogeneity of lower limb EMG patterns during pedaling (Ryan and Gregor 1992; Hug et al. 2004). Hug et al. (2004) did not report EMG profiles in respect to the crank cycle. In contrast, Ryan and Gregor (1992) depicted EMG profiles in ten lower limb muscles but did not provide a precise description of the training/physiological status of the subjects. Overall, our results are in accordance with those previously reported (Ryan and Gregor 1992; Hug et al. 2004) showing a high variability for biarticular muscles, especially for RF and GL. However, in contrast to Hug et al. (2004), we also reported a high variability for TA. This discrepancy could be explained by the fact that Hug et al. (2004) only reported information about the EMG activity level with respect to the crank cycle (they did not report EMG patterns). Thus, it could be hypothesized that TA variability is mainly linked to differences in shape and timing of the individual EMG patterns. In support of this idea, Ryan and Gregor (1992) reported and discussed three separate TA patterns. We also found highly different individual patterns for this muscle as shown in the example depicted in Fig. 6.

Our results confirmed that the EMG patterns of monoarticular muscles (with the exception of TA) are less variable: VL and VM are the lowest variable muscles at 150 W, while GMax is the lowest variable muscle at 250 W. It confirms that the GMax activity would be greatly influenced by workload level as suggested by Ericson (1986). The low variability of these monoarticular muscles could be explained by their role as primary power producers during pedaling (van Ingen Schenau et al. 1992). In contrast, according to the theory proposed by these authors, biarticular muscles appear to be active to transfer energy between joints at critical times in the pedaling cycle and to control the direction of force production. Thus, this high interindividual variability of EMG patterns reported in

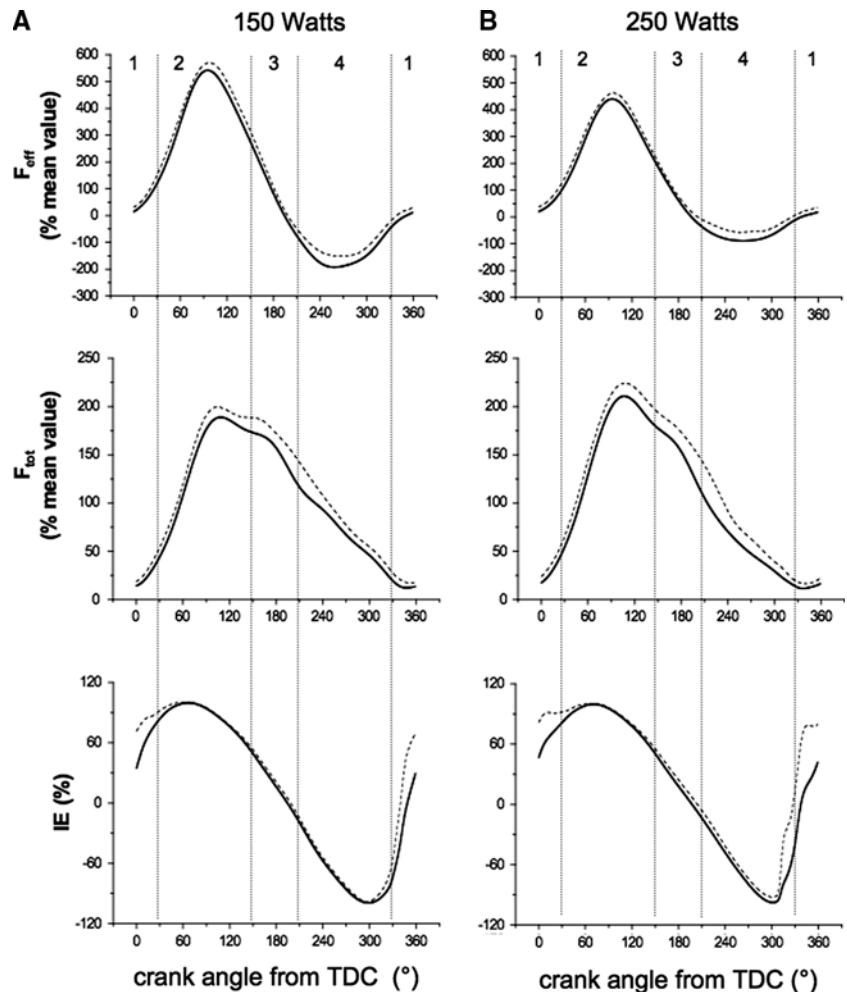
Table 2 Inter-individual variability of EMG RMS patterns at four angular sectors for the ten muscles at both exercise intensities [(a) 150 W and (b) 250 W]

	TA	SOL	GL	GM	VL	RF	VM	BF	SM	GMax
(a) 150 W										
VR sector 1	0.966	–	–	–	0.353	1.358	0.470	–	–	0.684
VR sector 2	0.620	0.244	0.318	0.166	0.283	0.862	0.222	0.546	0.358	0.341
VR sector 3	0.900	0.430	0.551	0.397	–	–	–	0.547	0.356	–
VR sector 4	0.871	0.525	0.667	0.565	–	0.744	–	0.576	–	–
(b) 250 W										
VR sector 1	0.952	–	–	–	0.305	1.363	0.453	–	–	–
VR sector 2	0.537	0.242	0.309	0.189	0.384	0.822	0.308	0.459	0.443	0.185
VR sector 3	0.768	0.507	0.548	0.391	–	–	–	0.673	0.382	–
VR sector 4	0.864	1.089	0.615	0.578	–	0.582	–	0.521	0.666	–

Omitted values appear when the mean activity over a sector was considered as negligible (i.e., <10% of the maximal activity over the complete cycle)

VR variance ratio, GMax gluteus maximus, SM semimembranosus, BF biceps femoris, VM vastus medialis, RF rectus femoris, VL vastus lateralis, GM gastrocnemius medialis, GL gastrocnemius lateralis, SOL soleus, TA tibialis anterior

Fig. 7 Interindividual variability of effective force (F_{eff}), total force (F_{tot}) and index of mechanical effectiveness (IE) profiles at both exercise intensities (**a** 150 W, **b** 250 W). Vertical lines define the four angular sectors: sector 1 (330°–30°), sector 2 (30°–150°), sector 3 (150°–210°), sector 4 (210°–330°)



biarticular muscles in the present study appeared to support the contention suggested by these authors that the role of “fine tuning” the system and distributing energy among the

segments of these muscles would lead to more variance. Note that the ankle is not considered as a major power-producing joint and TA has been proposed to enhance

ankle function in transmitting power to the crank (Ryan and Gregor 1992); therefore, this could explain the high variability found in this monoarticular muscle. Overall and consistent with the theory of van Ingen Schenau et al. (1992), one may wonder whether high interindividual variability of the EMG patterns reported in biarticular muscles could be linked to a variability in the direction of force vector on the pedals, and thus maybe to a heterogeneity of the mechanical effectiveness.

Pedal force profiles

To the best of our knowledge, this is the first study to focus on intersubject variability in pedal effective force, total force and IE profiles. Our results suggest a low intersubject variability corresponding with high cross-correlation coefficients and relatively low MD and VR values for F_{eff} , F_{tot} and IE profiles computed across the whole pedaling cycle (Table 3). Detailed analysis of the different sectors highlights the consistency in all the pedal mechanical variables during the major propulsive phase (sector 2). In the same way, the next part of the cycle (sector 3: BDC) is also consistent regarding F_{eff} and IE even if the F_{tot} demonstrated high variability. An important finding is the great variability in F_{eff} and F_{tot} during the upstroke phase (sector 4) supporting the assumption that effective force profiles for this period appear as individual like fingerprints for each subject (Kautz et al. 1991). This variability was also evident, although to a lesser extent, for F_{eff} and F_{tot} in the last sector (sector 1: TDC) and was associated with high variability in IE. Finally, our results show a greater variability in the pedaling technique at 250 W compared to 150 W (i.e., higher IE variability on the complete cycle, Table 3, Fig. 7; higher variability of F_{eff} and IE in sectors 1 and 4, Table 4). This result supports the hypothesis that a greater power output could lead to an increased variability specifically during the upstroke and TDC phases (Sanderson 1991).

EMG versus pedal force variability

Consistency in the pedal mechanical variables during sector 2 is in strong agreement with the fact that this sector is characterized by a low variability in EMG activation patterns especially obtained for the main power producer muscles (VL, VM, GMax). The relative variability in sectors 1 and 4 can also be interpreted in the context of the EMG results. Indeed, it is interesting to note that sector 1 is characterized by highest variability in both EMG and mechanical patterns. The most probable explanation would be the link around the TDC between the activation strategy of TA and RF muscles and the ability of subjects to effectively orientate the force and hence produce a high

Table 3 Inter-individual variability of complete cycle effective force (F_{eff}), total force (F_{tot}) and index of mechanical effectiveness (IE) profiles at both exercise intensities [(a) 150 W and (b) 250 W]

	F_{eff}	F_{tot}	IE
(a) 150 W			
MD (%)	30.3	12.2	7.7
VR	0.017	0.047	0.037
\overline{R}_0	0.988	0.987	0.962
(b) 250 W			
MD (%)	23.6	15.3	12.4
VR	0.019	0.059	0.088
\overline{R}_0	0.987	0.982	0.922

MD mean deviation, VR variance ratio, \overline{R}_0 cross-correlation coefficient

Table 4 Inter-individual variability of effective force (F_{eff}), total force (F_{tot}) and index of mechanical effectiveness (IE) profiles at four angular sectors at both exercise intensities [(a) 150 W and (b) 250 W]

	F_{eff}	F_{tot}	IE
(a) 150 W			
VR sector 1	0.197	0.359	0.243
VR sector 2	0.071	0.063	0.000
VR sector 3	0.064	0.547	0.005
VR sector 4	0.444	0.204	0.002
(b) 250 W			
VR sector 1	0.291	0.243	0.253
VR sector 2	0.058	0.086	0.000
VR sector 3	0.059	0.556	0.007
VR sector 4	0.699	0.366	0.036

VR variance ratio

F_{eff} in this specific part of the cycle. The relationship is however less consistent around BDC (i.e., medium to high variability of BF, GL and TA versus negligible variability of F_{eff} and IE). Additionally, to attribute the great variability in mechanical parameters during the upstroke phase to the variability in EMG remains debatable when considering the very low global muscle activity level during this period. Furthermore, the functional role of the muscles, which are slightly activated during this sector, remains to be elucidated. As a whole, the relative variability in sectors 1 and 4, when the level of force is low, seems not to have a great impact on the intersubject variability calculated across the whole cycle. However, the implications of such variations should not be ignored in the context of long duration cycling exercises.

The difference in variability between pedal force and EMG (i.e., low variability of the mechanical variables

compared to EMG) could be explained by the fact that the musculoskeletal system has the characteristics of a low-pass filter. Although the myoelectrical signal has frequency components over 100 Hz, the force signal is of much lower frequencies (i.e., muscle force profiles are smoother than raw EMG profiles). There are many mechanisms that may cause this filtering, like excitation–contraction coupling and muscle/tendon viscoelasticity. However, for the EMG signal to be correlated with the muscle force, and as recommended by various authors (Buchanan et al. 2004), we used an EMG processing that permits to filter out the high-frequency components. Even if it is not possible to be sure that the filtering is sufficient, we think that the more plausible explanation for the difference in variability between pedal force and EMG is the redundancy of the neuromuscular system. In fact, lower limbs have more muscles than joints such that the same pedal force profile can be produced by various lower limb muscle patterns. Associated with the reproducibility of the EMG patterns during pedaling showed by Dorel et al. (2008b), our result suggests that each cyclist adopts a stable personal muscle activation strategy. However, some questions remain to be answered: how a muscle coordination pattern is selected from a large pool of valid alternatives? Is there an optimal coordination pattern or do the cyclists adopt their personal optimal coordination pattern?

Conclusion

This study shows high intersubject variability of EMG patterns at both exercise intensities (i.e., 150 and 250 W), especially for biarticular muscles. It suggests that despite their high and homogeneous level of expertise, cyclists adopt a personal muscle activation strategy during pedaling. However, this heterogeneity of EMG patterns is not accompanied by a so high intersubject variability in pedal force application patterns. Even if variability in EMG patterns is in line with the slight variability of the mechanical parameters observed during the upstroke phase and around the top dead center, the results of this work highlight that the flexibility at the muscle level as a whole is greater than that seen in the net effective torque that muscles induce at the level of the crank. Overall, these results provide additional evidence for redundancy in the neuromuscular system: the neuromuscular system has multiple ways of accomplishing a given motor task.

Acknowledgments This study was funded in part by “La fondation d’entreprise de la Française Des Jeux” and the French Ministry of Sport (contract no. 06-046). The authors are grateful for the subjects for having accepted to participate in this study.

References

- Bernstein N (1967) Coordination and regulation of movements. Pergamon Press, New York
- Buchanan TS, Lloyd DG, Manal K, Besier TF (2004) Neuromusculoskeletal modeling: estimation of muscle forces and joint moments and movements from measurements of neural command. *J Appl Biomech* 20:367–395
- Burden AM, Trew M, Baltzopoulos V (2003) Normalisation of gait EMGs: a re-examination. *J Electromyogr Kinesiol* 13:519–532. doi:10.1016/S1050-6411(03)00082-8
- Cavanagh PR, Komi PV (1979) Electromechanical delay in human skeletal muscle under concentric and eccentric contractions. *Eur J Appl Physiol Occup Physiol* 42:159–163. doi:10.1007/BF00431022
- Chapman AR, Vicenzino B, Blanch P, Hodges PW (2007) Patterns of leg muscle recruitment vary between novice and highly trained cyclists. *J Electromyogr Kinesiol* 18(3):359–371
- Dal Monte A, Manoni A, Fucci S (1973) Biomechanical study of competitive cycling: the forces exercised on the pedals. In: Press B (ed) *Biomechanics III*. pp 434–439
- Dingwell JB, Ulbrecht JS, Boch J, Becker MB, O’Gorman JT, Cavanagh PR (1999) Neuropathic gait shows only trends towards increased variability of sagittal plane kinematics during treadmill locomotion. *Gait Posture* 10:21–29. doi:10.1016/S0966-6362(99)00016-8
- Dorel S, Couturier A, Hug F (2008a) Influence of different racing positions on mechanical and electromyographic patterns during pedalling. *Scand J Med Sci Sports* (in press)
- Dorel S, Couturier A, Hug F (2008b) Intra-session repeatability of lower limb muscles activation pattern during pedaling. *J Electromyogr Kinesiol* (in press)
- Ericson M (1986) On the biomechanics of cycling. A study of joint and muscle load during exercise on the bicycle ergometer. *Scand J Rehabil Med Suppl* 16:1–43
- Gregor RJ, Cavanagh PR, LaFortune M (1985) Knee flexor moments during propulsion in cycling—a creative solution to Lombard’s Paradox. *J Biomech* 18:307–316. doi:10.1016/0021-9290(85)90286-6
- Gregor RJ, Komi PV, Browning RC, Jarvinen M (1991) A comparison of the triceps surae and residual muscle moments at the ankle during cycling. *J Biomech* 24:287–297. doi:10.1016/0021-9290(91)90347-P
- Hermens HJ, Freriks B, Disselhorst-Klug C, Rau G (2000) Development of recommendations for SEMG sensors and sensor placement procedures. *J Electromyogr Kinesiol* 10:361–374. doi:10.1016/S1050-6411(00)00027-4
- Hug F, Dorel S (2008) Electromyographic analysis of pedaling: a review. *J Electromyogr Kinesiol* (in press)
- Hug F, Bendahan D, Le Fur Y, Cozzone PJ, Grelot L (2004) Heterogeneity of muscle recruitment pattern during pedaling in professional road cyclists: a magnetic resonance imaging and electromyography study. *Eur J Appl Physiol* 92:334–342. doi:10.1007/s00421-004-1096-3
- Hull ML, Davis RR (1981) Measurement of pedal loading in bicycling: I. Instrumentation. *J Biomech* 14:843–856. doi:10.1016/0021-9290(81)90012-9
- Kautz SA, Feltner ME, Coyle EF, Baylor AM (1991) The pedaling technique of elite endurance cyclists: changes with increasing workload at constant cadence. *Int J Sport Biomech* 7:29–53
- LaFortune MA, Cavanagh PR (1983) Effectiveness and efficiency during cycling riding. In: *Biomechanics VIII-B: international series on biomechanics*. Human Kinetics. pp 928–936
- Li L, Caldwell GE (1999) Coefficient of cross correlation and the time domain correspondence. *J Electromyogr Kinesiol* 9:385–389. doi:10.1016/S1050-6411(99)00012-7

- Mirka GA (1991) The quantification of EMG normalization error. *Ergonomics* 34:343–352. doi:[10.1080/00140139108967318](https://doi.org/10.1080/00140139108967318)
- Rouffet DM, Hautier CA (2008) EMG normalization to study muscle activation in cycling. *J Electromyogr Kinesiol* (in press)
- Rowe T, Hull ML, Wang EL (1998) A pedal dynamometer for off-road bicycling. *J Biomech Eng* 120:160–164. doi:[10.1115/1.2834297](https://doi.org/10.1115/1.2834297)
- Ryan MM, Gregor RJ (1992) EMG profiles of lower extremity muscles during cycling at constant workload and cadence. *J Electromyogr Kinesiol* 2:69–80. doi:[10.1016/1050-6411\(92\)90018-E](https://doi.org/10.1016/1050-6411(92)90018-E)
- Sanderson DJ (1991) The influence of cadence and power output on the biomechanics of force application during steady-rate cycling in competitive and recreational cyclists. *J Sports Sci* 9:191–203
- Sanderson DJ, Black A (2003) The effect of prolonged cycling on pedal forces. *J Sports Sci* 21:191–199. doi:[10.1080/0264041031000071010](https://doi.org/10.1080/0264041031000071010)
- Sanderson DJ, Hennig EM, Black AH (2000) The influence of cadence and power output on force application and in-shoe pressure distribution during cycling by competitive and recreational cyclists. *J Sports Sci* 18:173–181. doi:[10.1080/026404100365072](https://doi.org/10.1080/026404100365072)
- Shan G (2008) Biomechanical evaluation of bike power saver. *Appl Ergon* 39:37–45
- Shiavi R, Bourne J, Holland A (1986) Automated extraction of activity features in linear envelopes of locomotor electromyographic patterns. *IEEE Trans Biomed Eng* 33:594–600. doi:[10.1109/TBME.1986.325841](https://doi.org/10.1109/TBME.1986.325841)
- Shiavi R, Bugle HJ, Limbird T (1987) Electromyographic gait assessment, Part 1: adult EMG profiles and walking speed. *J Rehabil Res Dev* 24:13–23
- van Bolhuis BM, Gielen CC (1999) A comparison of models explaining muscle activation patterns for isometric contractions. *Biol Cybern* 81:249–261. doi:[10.1007/s004220050560](https://doi.org/10.1007/s004220050560)
- van Ingen Schenau GJ, Boots PJM, de Groot G, Snackers RJ, van Woensel WWLM (1992) The constrained control of force and position in multi-joint movements. *Neuroscience* 46:197–207. doi:[10.1016/0306-4522\(92\)90019-X](https://doi.org/10.1016/0306-4522(92)90019-X)
- Vos EJ, Mullender MG, van Ingen Schenau GJ (1990) Electromechanical delay in the vastus lateralis muscle during dynamic isometric contractions. *Eur J Appl Physiol Occup Physiol* 60:467–471. doi:[10.1007/BF00705038](https://doi.org/10.1007/BF00705038)
- Winter DA, Yack HJ (1987) EMG profiles during normal human walking: stride-to-stride and inter-subject variability. *Electroencephalogr Clin Neurophysiol* 67:402–411. doi:[10.1016/0013-4694\(87\)90003-4](https://doi.org/10.1016/0013-4694(87)90003-4)
- Wren TA, Do KP, Rethlefsen SA, Healy B (2006) Cross-correlation as a method for comparing dynamic electromyography signals during gait. *J Biomech* 39:2714–2718. doi:[10.1016/j.jbiomech.2005.09.006](https://doi.org/10.1016/j.jbiomech.2005.09.006)
- Yang JF, Winter DA (1984) Electromyographic amplitude normalization methods: improving their sensitivity as diagnostic tools in gait analysis. *Arch Phys Med Rehabil* 65:517–521